EG UK Computer Graphics & Visual Computing (2018)
G. Tam and F. Vidal (Editors)

Topological connected chain modelling for classification of mammographic microcalcification

M. George[1], E. R. E Denton[2] and R. Zwiggelaar[1]

[1]Department of Computer Science, Aberystwyth University, Aberystwyth, SY23 3DB, UK
{mig24, rrz}@aber.ac.uk
[2]Department of Breast Imaging, Norfolk and Norwich University Hospital, Norwich NR4 7UY,UK
erika.denton@nnuh.nhs.uk

Abstract

Breast cancer continues to be the most common type of cancer among women. Early detection of breast cancer is key to effective treatment. The presence of clusters of fine, granular microcalcifications in mammographic images can be a primary sign of breast cancer. The malignancy of any cluster of microcalcification cannot be reliably determined by radiologists from mammographic images and need to be assessed through histology images. In this paper, a novel method of mammographic microcalcification classification is described using the local topological structure of microcalcifications. Unlike the statistical and texture features of microcalcifications, the proposed method focuses on the number of microcalcifications in local clusters, the distance between them, and the number of clusters. The initial evaluation on the Digital Database for Screening Mammography (DDSM) database shows promising results with 86% accuracy and findings which are in line with clinical perception of benign and malignant morphological appearance of microcalcification clusters.

CCS Concepts

•***Keywords*** → *microcalcification classification, benign/malignant, topological modelling, graph connected chain;*

1. Introduction

Breast cancer is the most common cause of cancer death among women worldwide [SMJ16]. Early detection and timely treatment is the most effective way to reduce mortality. A variety of medical imaging techniques are available for monitoring abnormalities in breast tissue including ultrasound and magnetic resonance imaging but mammography is the most frequently used for initial cancer detection. Mammography can identify some abnormalities before they are detectable physically. Breast cancer can appear in mammograms as masses, architectural distortions or microcalcifications. Masses appear as large white bright regions in mammograms while, microcalcifications are bright, small in size and form clusters. Breast microcalcifications are small spots of calcium deposits which are common among women and are mostly benign [CCC*03], with some examples shown in Figure 1. The presence of fine, patterned granular microcalcification clusters can be an indication of early breast carcinoma requiring histological examination for confirmation.These can be classified as benign or malignant based on their size, shape, form, number, density, distribution area and margins.

Computer-aided diagnosis (CAD) can provide an alternative to double reading of mammograms or assist the reader in abnormality detection using advanced computer algorithms [Nis07]. Although

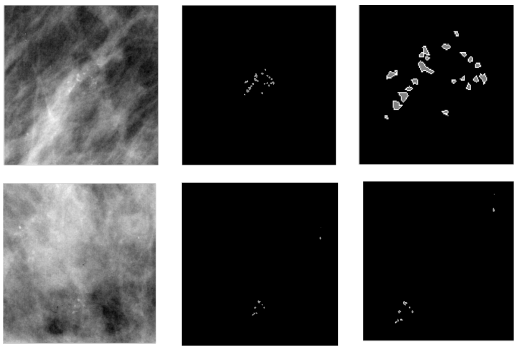

Figure 1: *Examples of ROI patches of malignant (top row) and benign (bottom row) mammographic microcalcification clusters, First column: original patch; second column: annotated microcalcifications; third column: zoomed in view of microcalcifications.*

CAD systems help in the early detection of many breast abnormalities, the interpretation/classification of microcalcifications remains difficult due to: (a) their small size, (b) although high contrast there is potential overlap with dense tissue, and (c) the absence of par-

DOI: 10.2312/cgvc.20181201

ticular patterns or templates due to the variation in sizes, shapes and distribution of microcalcification [CCC*03]. Enhancement and noise filtering can be beneficial for the localisation of microcalcifications in breast tissue [CCC*03]. CAD systems have two phases: a) detection and localization of the abnormality and b) classification of the abnormality as benign or malignant. Various features have been used to classify microcalcifications, for example individual microcalcification characteristics describing the perimeter, area, compactness, elongation, eccentricity, thickness, orientation, contrast [SPK06]. Other features used for classification includes co-occurrence features, wavelet properties, Gabor filter bank features, scale-space characteristics, fractal and cluster features [CCC*03], [EH92].

Analysing and extracting the features of detected microcalcifications is an important phase in a CAD system for the classification of the detected microcalcifications. Various features of microcalcification have been studied for classifying them as malignant or benign cases and here we provide an overview from the literature which we used as a source to identify features used in the developed approach. Elter and Horsch [EH92] described shape, size, cluster features, intensity, texture, morphology and topology features for classification of microcalcifications. Some of the wavelet features [DFR*08] used for classification included energy and entropy while the cluster features for classification described the distribution of local features, cluster area, cluster perimeter, cluster diameter, eccentricity, elongation and number of microcalcifications in the cluster representing the cluster morphology [BRW97].

According to breast microcalcifications studies, it is found that malignant microcalcifications tend to be small and densely distributed (>5 per focus within 1cm^2), while benign microcalcifications are usually larger, smaller in number and scattered (<4-5 per 1cm^2) [Sic86], [FGM87]. Estimating the distribution and closeness of microcalcification in the clusters, Chen et al. [CSO*15] proposed a topology-based classification method by constructing graphs at multiple scales. The graph features were estimated at different scales for the topological modelling and classification of microcalcification into benign and malignant cases. Similarly, Suhail et al. [SDZ18] used a tree based topological approach for the classification of microcalcification focusing on the distribution and connectivity of microcalcacification. The tree features like height of the tree and number of leaf nodes were evaluated for the classification process. Simultaneously, the deep learning techniques have been developed for classifying lesions in mammograms [BGG16].

This paper deals with the classification of manually or automatically detected microcalcification clusters as benign or malignant using topological features of the microcalcification clusters. Unlike the tree-based approach of Suhail et al. [SDZ18], the proposed method used the closeness and distribution of microcalcifications forming local clusters, and how the clusters are spread, which is linked to the clinical aspects in estimating the classification of microcalcifications. The evaluation was performed on the Digital Database for Screening Mammography (DDSM) dataset [HBK*98].

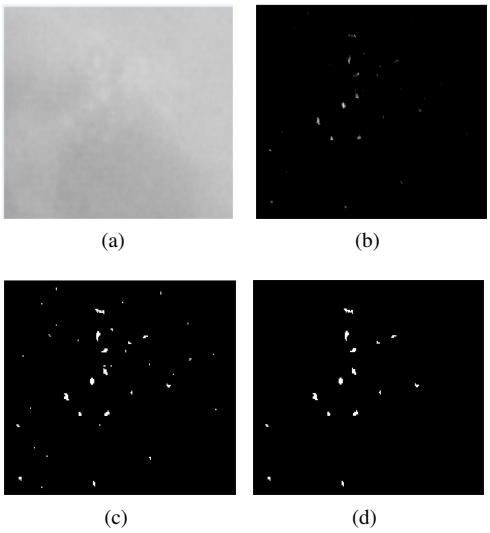

Figure 3: *Binarization and denoising of annotated microcalcification cluster; (a) original mammographic patch with microcalcification, (b) annotated microcalcification cluster image, (c) binarized image, (d) denoised image.*

2. Data and Methodology

In our study, the data used for microcalcification classification were mammograms from the DDSM dataset. A total of 289 mammogram ROIs of varied sizes with microcalcification abnormalities were evaluated, where 131 mammogram ROIs were histologically proven as malignant cases while 158 mammogram ROIs were histologically proven as benign cases. The average size of these ROIs was 482×450 pixels, though it should be mentioned that the proposed method is independent of the patch size.

The proposed approach used the clinical perspective that benign microcalcifications are of larger size and are more widely spread while malignant microcalcifications are smaller and more closely distributed. A detailed overview of the proposed method is illustrated in Figure 2.

In the proposed approach, the segmented image ROIs with microcalcification are automatically annotated using the detection method of Oliver et al. [OTL*12]. Subsequently, the annotated mammogram ROIs are binarized by converting to binary images. All the pixels with value '0' represented background or normal tissue while the pixels with value '1' indicated microcalcifications. Single and low probability pixels were removed as they were considered as noise. So, the denoising was performed by removing low probability pixels and by deleting small areas with size smaller than 4 pixels as shown in Figure 3, which demonstrates the initial steps of automatic localisation, binarization and denoising of image ROIs.

After the pre-processing, the centroids of each microcalcifications were estimated. Thereafter the distance between each centroid point was calculated to estimate their relative position. To estimate the connectivity between the microcalcifications, connected

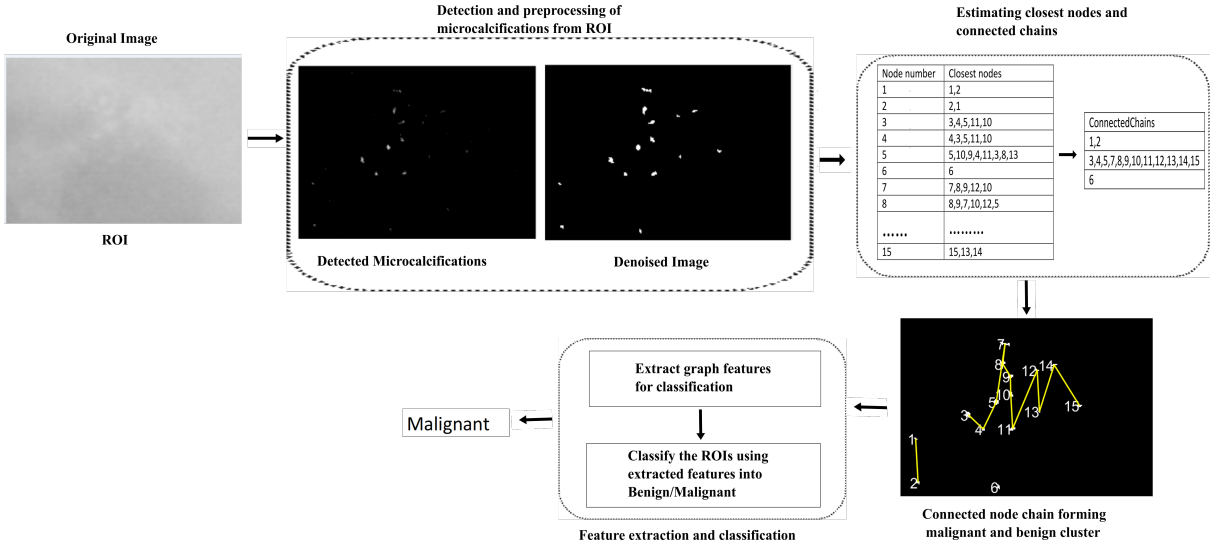

Figure 2: *Detailed representation of the proposed connected chain graph method for microcalcification classification into benign/malignant.*

chains were constructed. Connected node chains were estimated using a threshold distance of 40 pixels to estimate the longest possible connected chain. The connected node chains were constructed by closely estimating and joining the nodes which are distributed within 40 pixels around each node. The first node was taken and the next closest node to it from the distance map was joined with it, followed by the nearest node to the previously connected node. The procedure was continued till there was no unconnected close nodes to any of the nodes in the constructed chain. The procedure continued by selecting the next unvisited node from the node list to start the next chain. So, each connected chain represented a cluster of microcalcifications. The method is illustrated in Figure 4. The connected nodes in the chain show the pattern of node arrangement in that cluster, which was the representation of closely located connected nodes. In other words, the number of connected chains represent the independent number of cluster. Those microcalcifications which are closely located will form a cluster (3,4,5,7,8,9,10,11,12,13,14,15), (1,2) while scattered microcalcifications are considered as unvisited or leaf nodes (6) as shown in Figure 4.

For feature extraction of the clusters, the cluster properties calculated were the number of clusters, the number of benign clusters (the chains containing less than or equal to 5 nodes), the number of malignant clusters (the chains with more than 5 nodes), the size of the longest chain, the number of independent nodes/leaf nodes. Figure 5 illustrates the difference between connected chains formed for benign and malignant cases. The first column represents the mammographic patch while the second column shows the segmented and annotated calcifications and the third column represent the connected chains for benign and malignant cases. The structure of connected chains for malignant microcalcifications is complex compared to the benign structure as the malignant microcalcificatios are closely and densely arranged giving a long dense chain.

The classification of mammographic ROIs into benign and malignant cases using the topological features extracted from clusters were evaluated using the Bayesian network and k-nearest neighbours (kNN) classifiers. The classical kNN classifier is an instance - based learning approach. We used the kNN classifier as most of the literature use the classical kNN approach for the classification. It is based on simple majority voting unless equal class probability is indicated, and the Euclidean weighted approach is used as the distance measure. Similarly, a Bayesian network was also used as a classifier for comparison and it used a simple hill climbing algorithm for the classification.

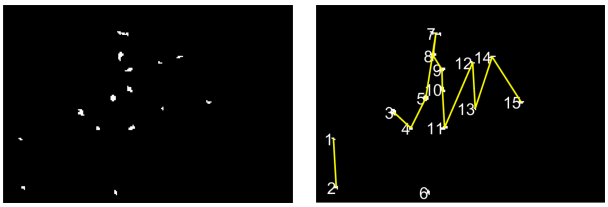

Figure 4: *Generating connected chains for microcalcifications to construct clusters, (a) the microcalcifications after denoising, (b) representing the cluster/connected node chain, which indicates three clusters of various sizes.*

3. Experimental Evaluation

To evaluate the performance of features extracted through the construction of connected chains by the mentioned classifiers, ten-fold cross-validation (10-FCV) and leave-one-out approaches were used for the DDSM dataset. The classification results using a Bayesian network using 10-FCV provided a classification accuracy of 85.5%. The confusion matrix shown in Table 1 shows the benign and malignant cases obtained by the classifier.

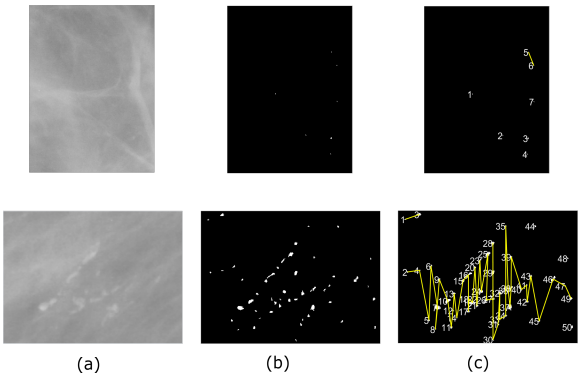

Figure 5: *Complexity representation of benign (top row) and malignant (bottom row) example ROIs. (a): original mammogram ROI; (b): the detected binarized microcalcification; (c): connected node chain for benign and malignant clusters.*

Table 1: *Confusion matrix for automatic classification using a Bayesian Network.*

		Automatic Classification	
		Benign	**Malignant**
Truth Data	**Benign**	144	14
	Malignant	28	103

Similarly, the kNN classifier (k=12) gave an accuracy of 82.7% on classifying the set of mammographic data. The results are illustrated in Table 2.

Table 2: *Confusion matrix for automatic classification using a classical kNN classifier.*

		Automatic Classification	
		Benign	**Malignant**
Truth Data	**Benign**	145	13
	Malignant	37	94

To evaluate and compare the effect of the leave-one-out approach, we compared the results obtained through both leave-one-out approach and 10-FCV for the Bayesian and kNN classifiers. The results were approximately the same in both cases as shown in Table 3.

A comparative study with other classifiers was also done for the evaluation of the proposed method. The evaluation results show that the proposed method is robust irrespective of the classifier. The comparative results for different classifiers using the 10-FCV and leave-one-out approaches are illustrated in Table 3.

The Bayesian Network was found to be the best with the extracted features for benign and malignant classification.

Based on the literature, the results are comparable with the results obtained by Chen et al. [CSO*15] using multiscale graph modelling of 86.5% for a subset of 160 ROIs without feature selection and Suhail et al. [SDZ18] with a classification accuracy of

Table 3: *Comparison of classification accuracy using different classifiers .*

		Automatic Classification	
		Leave-one-out	**10-FCV**
Truth Data	**Bayesian**	84.8	85.5
	kNN	83.0	82.7
	J48	82.0	82.7
	oneR	83.0	82.7

91% using multiscale tree modelling on the subset of 129 ROIs of the DDSM dataset.

Though the proposed approach can classify most of the cases correctly, there are misclassified instances like the ROIs shown in Figure 6. The top row ROI was misclassified as a benign case by the proposed approach where it only has one connected chain with less than 6 nodes and the other nodes are scattered giving less probability of malignancy. The second row was misclassified as malignant because of the large number of connected chains though the complexity of each connected chain is low giving an assumption of malignancy even when the microcalcifications were spread out over the patch.

4. Conclusion and Future Work

Detection and classification of benign and malignant microcalcifications is an important issue for CAD systems as it assists in the early diagnosis and treatment of breast cancer. CAD systems with great accuracy for detection and classification can act as a second reader of mammogram images.

In this paper we have introduced a novel approach considering the topological distribution of microcalcifications in mammogram ROIs. It has taken the clinical description of distance distribution into account for cluster classification processing. The results obtained using the proposed method are comparable with existing techniques from the literature.

The proposed algorithm was implemented at a specific scale and will be extended into a multi-scale approach to improve accuracy and to analyse the distribution of microcalcification in the clusters. In addition to the features extracted in this paper, more cluster, graph and other microcalcification features will be extracted to estimate the best features suitable for microcalcification classification as benign versus malignant. Similarly, the potential of tree models like minimum spanning trees will be studied to estimate their scope of topology features for classification. To investigate the efficiency of the proposed algorithm, additional datasets will be considered in the future.

References

[BGG16] BEKKER A. J., GREENSPAN H., GOLDBERGER J.: A multi-view deep learning architecture for classification of breast microcalcifications. In *Biomedical Imaging (ISBI), 2016 IEEE 13th International Symposium on* (2016), IEEE, pp. 726–730. 2

[BRW97] BETAL D., ROBERTS N., WHITEHOUSE G.: Segmentation and numerical analysis of microcalcifications on mammograms using

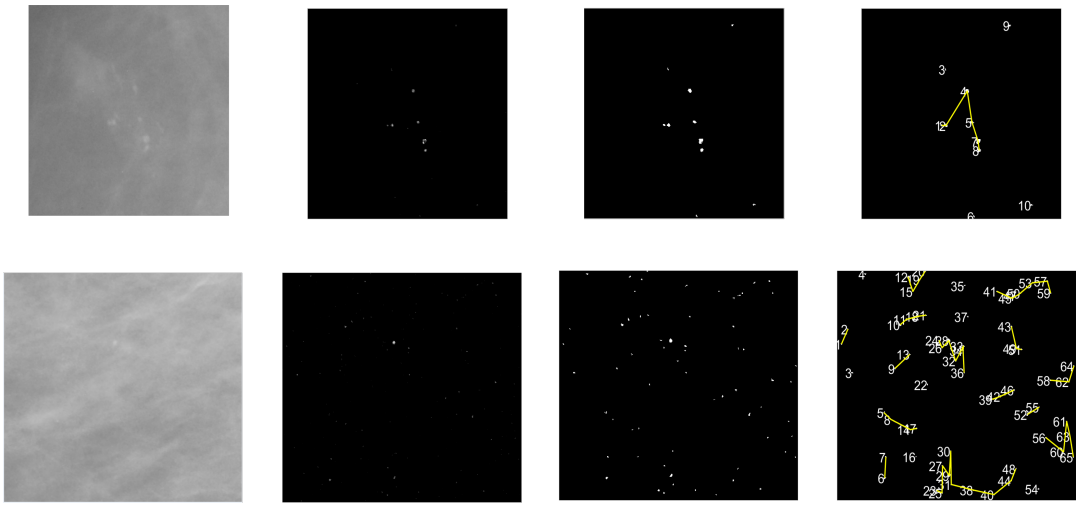

Figure 6: *Misclassified examples. First row: a malignant ROI reported as benign; Second row: benign ROI reported as malignant*

mathematical morphology. *The British Journal of Radiology 70*, 837 (1997), 903–917. 2

[CCC*03] CHENG H.-D., CAI X., CHEN X., HU L., LOU X.: Computer-aided detection and classification of microcalcifications in mammograms: a survey. *Pattern recognition 36*, 12 (2003), 2967–2991. 1, 2

[CSO*15] CHEN Z., STRANGE H., OLIVER A., DENTON E. R., BOGGIS C., ZWIGGELAAR R.: Topological modeling and classification of mammographic microcalcification clusters. *IEEE transactions on biomedical engineering 62*, 4 (2015), 1203–1214. 2, 4

[DFR*08] DOCUSSE T. A., FURLANI J. R., ROMANO R. P., GUIDO R. C., CHEN S.-H., MARRANGHELLO N., PEREIRA A. S.: Microcalcification enhancement and classification on mammograms using the wavelet transform. In *Neural Networks, 2008. IJCNN 2008.(IEEE World Congress on Computational Intelligence). IEEE International Joint Conference on* (2008), IEEE, pp. 3181–3186. doi:10.1109/IJCNN.2008.4634248. 2

[EH92] ELTER M., HORSCH A.: Cadx of mammographic masses and clustered microcalcifications: a review. *Medical Physics 36*, 6 (1992), 2052–2068. doi:10.1118/1.3121511. 2

[FGM87] FEIG S., GALKIN B., MUIR H.: Evaluation of breast microcalcifications by means of optically magnified tissue specimen radiographs. In *Breast Cancer*. Springer, 1987, pp. 111–123. 2

[HBK*98] HEATH M., BOWYER K., KOPANS D., KEGELMEYER P., MOORE R., CHANG K., MUNISHKUMARAN S.: Current status of the digital database for screening mammography. In *Digital mammography*. Springer, 1998, pp. 457–460. 2

[KLvG*17] KOOI T., LITJENS G., VAN GINNEKEN B., GUBERN-MÉRIDA A., SÁNCHEZ C. I., MANN R., DEN HEETEN A., KARSSEMEIJER N.: Large scale deep learning for computer aided detection of mammographic lesions. *Medical image analysis 35* (2017), 303–312.

[Nis07] NISHIKAWA R. M.: Current status and future directions of computer-aided diagnosis in mammography. *Computerized Medical Imaging and Graphics 31*, 4-5 (2007), 224–235. 1

[OTL*12] OLIVER A., TORRENT A., LLADÓ X., TORTAJADA M., TORTAJADA L., SENTÍS M., FREIXENET J., ZWIGGELAAR R.: Automatic microcalcification and cluster detection for digital and digitised mammograms. *Knowledge-Based Systems 28* (2012), 68–75. 2

[SDZ18] SUHAIL Z., DENTON E. R., ZWIGGELAAR R.: Tree-based modelling for the classification of mammographic benign and malignant micro-calcification clusters. *Multimedia Tools and Applications 77*, 5 (2018), 6135–6148. 2, 4

[Sic86] SICKLES E. A.: Breast calcifications: mammographic evaluation. *Radiology 160*, 2 (1986), 289–293. 2

[SMJ16] SIEGEL R. L., MILLER K. D., JEMAL A.: Cancer statistics, 2016. *CA: a cancer journal for clinicians 66*, 1 (2016), 7–30. 1

[SPK06] SAKKA E., PRENTZA A., KOUTSOURIS D.: Classification algorithms for microcalcifications in mammograms. *Oncology reports 15*, 4 (2006), 1049–1055. 2